Hebbian modification of a hippocampal population pattern in the rat

Charles King, Darrell A. Henze, Xavier Leinekugel and György Buzsáki

Center for Molecular and Behavioural Neuroscience, Rutgers, The State University of New Jersey, 197 University Avenue, Newark, NJ 07102, USA

(Received 1 March 1999; accepted after revision 25 August 1999)

1. The study of the physiological role of long-term potentiation (LTP) is often hampered by the challenge of finding a physiological event that can be used to assess synaptic strength. We explored the possibility of utilising a naturally occurring event, the hippocampal sharp wave (SPW), for the assessment of synaptic strength and the induction of LTP *in vivo*.

2. We used two methods in which hippocampal cells were either recorded intracellularly or extracellularly *in vivo*. In both cases, a linear association between the magnitude of the SPW and cellular responsiveness was observed.

3. LTP was induced by depolarising cells during SPWs by either direct intracellular current injection or extracellular microstimulation adjacent to the cell body. Both of these approaches led to an increase in the slope of the linear association between SPWs and cellular responsiveness.

4. This change was achieved without a rise in overall cell excitability, implying that the synapses providing input to CA1 cells during sharp waves had undergone potentiation.

5. Our findings show that the Hebbian pairing of cellular activation with spontaneous, naturally occurring synaptic events is capable of inducing LTP.

It is widely postulated that long-term potentiation (LTP) serves as a model of synaptic plasticity and, by extension, the substrate of memory in the hippocampus (Bliss & Collingridge, 1993), though this issue is still the subject of much debate (Barnes, 1995; Stevens, 1998). In a typical potentiation protocol, synaptic strength is assessed by using electrical pulses applied to fibres that provide synaptic input to the cells being studied. Similarly, LTP is induced by either tetanising the synaptic inputs or repeated pairing of postsynaptic depolarisation with single activations of the synaptic inputs. However, it may be argued that the typical means of testing synaptic strength and inducing LTP are artificial. In the intact hippocampal network, hippocampal principal cells are strongly inhibited by the activity of interneurons. Since bulk stimulation of afferent fibres leads to an activation of both pyramidal cells and interneurons in a manner rarely, if ever, observed under physiological conditions, it is desirable to determine if the 'rules' of LTP, as determined for such evoked responses, also apply under physiological conditions (Stevens, 1998). This issue is especially challenging in the hippocampus as its cells do not respond to simple sensory input patterns (Ranck, 1973).

In the present paper, we used a naturally occurring hippocampal population pattern, the sharp wave burst (SPW) and its associated 200 Hz ripple, as a temporally discrete physiological signal to assess synaptic strength at the Schaffer collateral to CA1 pyramidal cell synapse. Hippocampal SPWs emerge in the CA3 collateral system. As a result of the CA3 population bursts, the Schaffer collaterals provide synaptic activation to both pyramidal cells and interneurons with a net gain of excitation in area CA1 (Buzsáki *et al.* 1983; Csicsvari *et al.* 1999). Thus we hypothesised that the synaptic efficacy of the CA3–CA1 afferents could be measured by simultaneously monitoring the synaptic input, as represented by population activity, and the postsynaptic responsiveness of single cells or a small population of pyramidal neurons.

The Hebbian form of LTP is dependent on the depolarisation of the postsynaptic cell concurrent with the activation of synaptic input to that cell (Kelso *et al.* 1986; Wigstrom *et al.* 1986; Brown *et al.* 1990). Thus, we also hypothesised that by pairing depolarisation and discharge of CA1 pyramidal cells with the occurrence of SPWs, we could increase the strength of the SPW-activated synaptic inputs to the activated cells. We accomplished such a pairing protocol by using the spontaneously occurring SPWs to trigger strong postsynaptic depolarisations of CA1 pyramidal cells. The necessary depolarisations were obtained by either direct current injection via an intracellular electrode or via extracellular microstimulation of a small group of neurons. Some of these results have been previously presented (King & Buzsáki, 1998).

METHODS

All animal experimentation was carried out in accordance with the guidelines laid down by Rutgers Laboratory Animal Services and the National Research Council Guide for the Care and Use of Laboratory Animals.

Intracellular experiments

The *in vivo* intracellular recording methods are detailed elsewhere (e.g. Ylinen *et al.* 1995). Briefly, all intracellular recordings were obtained from hippocampal area CA1 *in vivo* from Sprague–Dawley rats under urethane anaesthesia ($1{\cdot}5\ \mathrm{g\ kg^{-1}}$). All electrodes were placed stereotaxically (AP $= -3{\cdot}5$ mm, ML $= \pm 2{\cdot}5$ mm from bregma). Intracellular recordings were obtained using an Axoclamp-2A amplifier (Axon Instruments) in bridge mode. Sharp electrodes were filled with 1 M potassium acetate and 2% biocytin (final resistance 60–100 MΩ). All cells had resting potentials less than −55 mV (mean $= -68 \pm 0{\cdot}73$ mV S.E.M.; $n = 30$). Simultaneous extracellular recordings from the pyramidal layer near the intracellularly recorded cells were obtained using nickel–chromium wires that consisted of either a single 50 μm wire or a 'tetrode' of four 12·5 μm wires. Extracellular signals were amplified and filtered using a multichannel amplifier (Grass Instrument Co.). For the 'training' protocol, the extracellular signal was filtered between 300 and 3000 Hz and fed to a spike discriminator. The output of the spike discriminator was then integrated with a 100–200 ms time constant, amplified, and fed into the external command input of the Axoclamp amplifier. In five experiments, an analog delay of 50–2000 ms was introduced to dissociate the SPW-associated input and cellular depolarisation ('pseudotraining'). It was found that this system provided a controlled injection of depolarising current through the intracellular electrode that elicited bursts of action potentials that were time locked to the occurrence of SPWs.

Extracellular experiments

Adult Sprague–Dawley rats were used. During surgery, the animals were anaesthetised with a combination of ketamine ($75\ \mathrm{mg\ kg^{-1}}$), xylazine ($19\ \mathrm{mg\ kg^{-1}}$) and acepromazine ($0{\cdot}75\ \mathrm{mg\ kg^{-1}}$) I.M. and given supplements consisting of a third of the inital dose at intervals of approximately 1·5 h. The need for a supplement was assessed by monitoring the animals' corneal reflexes and responses to tail or paw pinch. The animals were implanted with two tetrodes fashioned from 12·5 μm wires each attached to an independently movable microdrive. One of the microdrives also carried a 50 μm tungsten wire for field recordings. All electrodes were gold-plated. The tetrodes were arranged so that the tips were spaced 150–300 μm apart (see Fig. 5*A*). The recorded signals were buffered by headstage amplifiers (unity gain) and filtered (units: 300–10 kHz; field: 1 Hz to 10 kHz). The headstage amplifier also provided input pins directly connected to the wires coming from the electrodes. Any two of the four wires could be used for stimulation. Each input of the headstage amplifiers was protected with two 6·2 V Zener diodes mounted in opposite polarity. The signals were digitised using an ISC-16 board (RC Electronics, Santa Barbara, CA, USA) mounted in an IBM-compatible PC. Sample intervals of 50 or 100 μs were used.

A Grass Model S48 stimulator was used together with a SIU5 isolation unit. The negative output from the isolator was connected to the electrode on which the cell(s) appeared largest, and which was therefore presumably closest to the cell body. This ensured that the neuron(s) closest to the recording wire could be stimulated with the lowest amount of current. The positive output was connected to either another electrode in the same bundle or to the head screw used as an indifferent reference. Stimulation consisted of 50 ms square-wave pulses, the amplitude of which was adjusted to ensure activation of the cell. The rats were allowed to move freely, but recordings were performed while the animal was asleep to ensure a steady succession of hippocampal ripple events.

The exact current delivered to the electrode was determined during the experiment for each rat. Before the animal was killed, the electrode impedance was measured by monitoring the voltage drop across a 2 MΩ resistor in series with the negative output of the isolator at different stimulator voltages. Following the experiment, the brain was perfused and processed with Nissl staining to verify the position of the electrodes. In both intra- and extracellular experiments the animals were killed by a parenteral overdose of urethane.

Data analysis

For analysis purposes, SPWs were detected based upon the occurrence of their associated high frequency ripples (Figs 1 and 2*A*). Broad-band (1–3000 Hz) extracellular signals were filtered between 100 and 250 Hz using a digital 5-pole Bessel filter then rectified and smoothed using a median smoothing algorithm. The occurrence of a ripple was determined based upon a deflection of the processed extracellular signal greater than seven standard deviations from the baseline. The start and end of the ripple were then determined from the closest zero values preceding and following the threshold crossing. The magnitude of the ripple was determined by integrating over the duration of each ripple. The intracellular correlates of the ripples were determined by integrating the intracellular signal over the same time range. The 'zero' value for the intracellular integration was determined by the average membrane potential in a 10 s period that included the ripple. Any spontaneous action potentials were digitally removed from the intracellular signal and replaced by 2 ms of the value at the threshold for the action potential. For the extracellular experiments, ripples were detected as described for the intracellular experiments. The magnitude of the ripple was correlated with the number of spikes recorded in the same time window. Spikes were detected by computing the root-mean square of the filtered signal and isolating those segments in which the power deviated from that of the baseline noise by more than five standard deviations. Extracellular spikes were clustered as described earlier (Csicsvari *et al.* 1998), based on analysis of the first three principal components of the waveforms. Because the identity of the activated units could not be determined exactly, the separated clusters were combined. Thus, the units presented here represent multiple unit activity recorded by a single tetrode. The experimental arrangement is illustrated in Fig. 1.

RESULTS

Intracellular experiments

As previously reported, SPWs are associated with a distinct depolarisation of pyramidal cell membrane potential (Ylinen *et al.* 1995). We have extended this observation by noting that the SPW-associated intracellular depolarisation has a time course which closely follows that of the local cellular activity, recorded extracellularly (Fig. 2*B*). It was found that the magnitude of the intracellular depolarisation varied as a function of the magnitude of the SPW ripples recorded extracellularly nearby. In 20 of the 30 cells tested, the correlation coefficient was $> 0{\cdot}5$. Following a 4–12 min baseline period, 4–8 min of 'training' were provided where strong depolarisation was paired with the spontaneously occurring SPWs ($52 \pm 5{\cdot}8$ pairings; $n = 28$ recordings). Following the training period, 4 min epochs were collected

at various times up to 50 min post-training. We found that this training protocol could induce a long-lasting increase in the magnitude of intracellular depolarisations associated with SPW ripples. This was reflected by the consistent increase in the slope of the relationship between the magnitude of the extracellular and intracellular SPW-associated signals. Figure 2*C* shows the results from a single experiment under control conditions and 20 min post-training. Training resulted in a larger depolarising response to the same physiological input (the SPW event) when compared to those recorded prior to training. Combined data from a total of 28 recordings are shown in Fig. 3. Note that the number of experiments contributing to each time point varied and the *N* values are indicated. The group data indicate that paired stimulation induced a significant increase in the magnitude of the synaptic response and that the effect lasted more than 15 min (Fig. 3; $P < 0{\cdot}05$; Wilcoxon signed ranks test). The variabilities in the slopes and difficulties in maintaining stable long-term intracellular recordings *in vivo* prevented accurate statistics on later time points. Nevertheless, the data support the conclusion that the potentiation effect lasted for up to an hour.

The training protocol did not lead to a change in overall cell excitability. This was determined by examining the number of spikes fired in response to a 350 ms 0·4 nA current step (pre-training: $9{\cdot}4 \pm 2{\cdot}5$; 6 min post-training: $9{\cdot}4 \pm 2{\cdot}6$; 18 min post-training: $9{\cdot}3 \pm 2{\cdot}8$). The threshold at which the first spike fired during the 0·4 nA current step showed a small, but non-significant, change (pre-training: $-58{\cdot}8 \pm 0{\cdot}7$ mV; 6 min post-training: $-57{\cdot}3 \pm 1{\cdot}04$ mV; 18 min post-training: $-56{\cdot}9 \pm 1{\cdot}2$ mV, $P > 0{\cdot}05$; Student's 2-tailed *t* test). Input resistance did show a significant change, rising from $27{\cdot}5 \pm 1{\cdot}2$ to $30{\cdot}7 \pm 1{\cdot}7$ MΩ after stimulation ($P < 0{\cdot}01$; Student's 2-tailed *t* test). While an increased input resistance might lead to an enhanced voltage response to an EPSC, the lack of any significant change in spike firing in reaction to an artificial current injection suggests that this did not confound the results.

In five control experiments, a 50–2000 ms delay was inserted between the ripple and postsynaptic depolarisation. The delayed training procedure ('pseudotraining') did not alter the relationship between the SPW-associated population discharge and intracellular SPW-associated signals (Fig. 4). Neither the resting membrane potential nor the input resistance of the recorded neurons changed significantly following delayed training.

Extracellular experiments

Because intracellular stimulation of a single neuron could not be achieved in freely moving animals we chose to use very low intensity microstimulation to activate a circumscribed group of cells. In this method, recording tetrodes were placed close to the cell bodies of pyramidal cells. The number of action potentials recorded by the

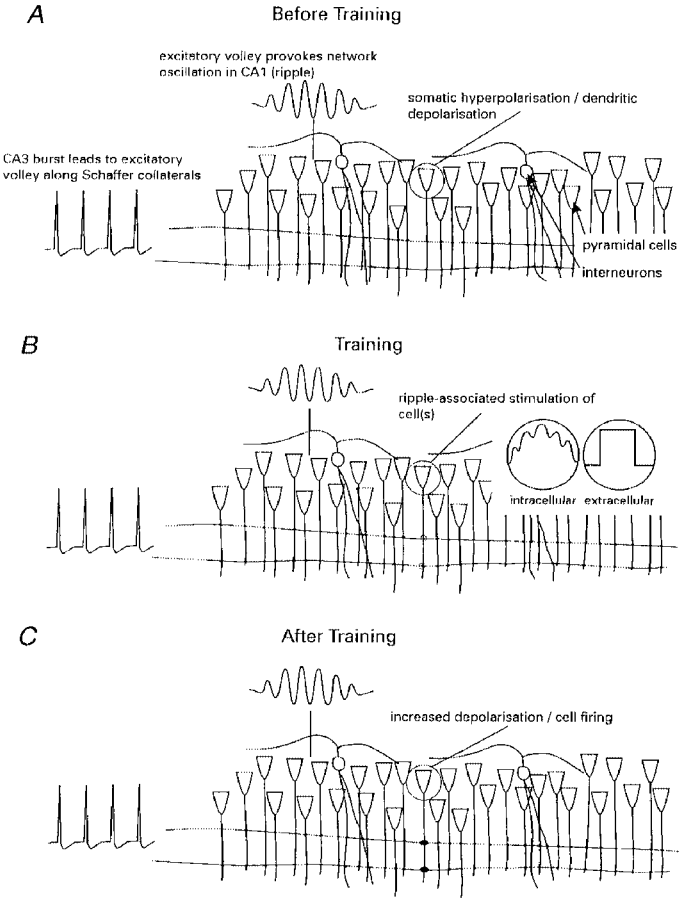

Figure 1. Schematics of the experimental rationale

Sharp wave (SPW) bursts are initiated in the CA3 region. *A*, the excitatory volleys of the Schaffer collaterals depolarise and discharge CA1 interneurons and pyramidal cells. The coherent discharge of interneurons produces a barrage of fast IPSPs in the somata of pyramidal cells, reflected as a fast field oscillation in the extracellular space (ripple). The ripple cycle-locked discharge of pyramidal neurons also contributes to the field ripple. Only 2–3 % of pyramidal cells discharge during a given ripple cycle. *B*, during training the rectified ripple (population signal) is fed back to an intracellularly recorded neuron to consistently depolarise and discharge it (intracellular). In the extracellular experiments the ripple signal triggers a 50 ms square wave pulse which is delivered to a small group of pyramidal cells by an extracellular electrode. *C*, after training the relationship between the extracellular ripple (population signal) and intracellular signal or local extracellular unit discharge is tested again.

tetrode was used to monitor cellular activity in the vicinity of the electrode. This measure was justified by our observations that the relationship between the number of spikes recorded from multiple cells was correlated linearly with the magnitude of the intracellular depolarisation of a single cell during the SPW event.

CA1 ripples exhibit a high degree of spatial coherence (Ylinen *et al.* 1995), indicating that they are the result of a network event reflecting activity extending far beyond the local areas of any one electrode. The size of the ripple is governed by two main factors: (1) coherent extracellular current flow from IPSPs in pyramidal cell somata, resulting

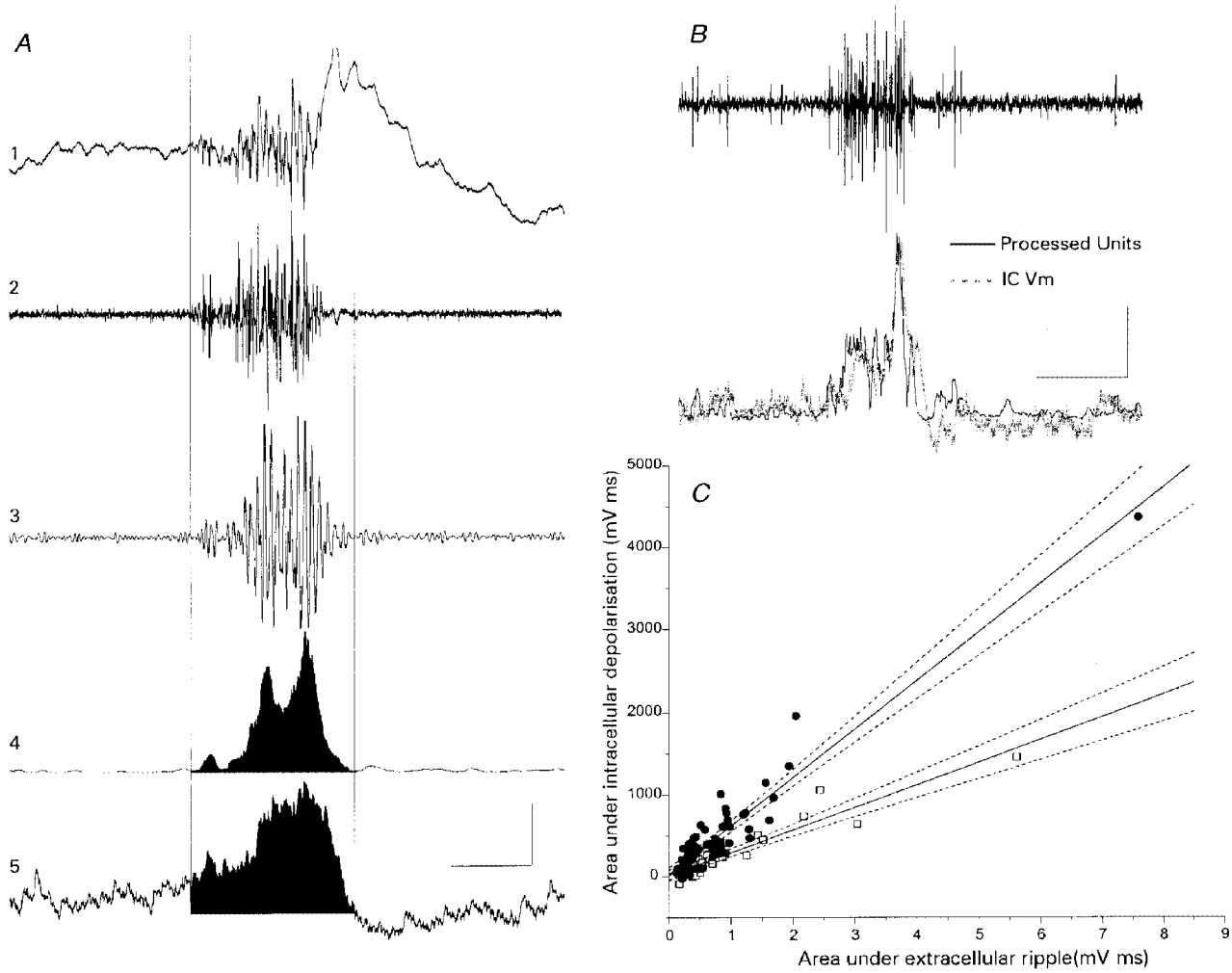

Figure 2. Detection and quantification of CA1 ripples and ripple-related intracellular potentials

A: trace 1, broad-band extracellular field (1–3000 Hz) recorded at the level of the pyramidal cell layer; trace 2, extracellular multiunit activity (trace 1 filtered to 300–3000 Hz); trace 3, SPW-related ripple (trace 1 filtered to 100–250 Hz); trace 4, rectified and smoothed SPW-associated ripple (trace 3 rectified and smoothed with a 100-point box car averager); trace 5, intracellular membrane potential changes associated with the ripple. The vertical lines indicate the duration of the ripple. The filled areas in traces 4 and 5 indicate the regions used to calculate the areas used for estimating the magnitude of the intracellular and extracellular ripple-related signals. The time scale is 100 ms and the amplitude scale is 0·25 mV in trace 1, 0·16 mV in trace 2, 0·09 mV in traces 3 and 4 and 5·0 mV in trace 5. *B*, example of the relationship between cellular activity measured extracellularly and intracellular membrane potential. The upper trace is an extracellular multiunit recording (filtered between 300 and 3 kHz; vertical scale: 0·12 mV). The lower trace consists of the rectified, smoothed, and scaled multiunit trace (continuous line) and a simultaneous intracellular recording of membrane potential (dotted line). The intracellular trace was recorded from a resting membrane potential of −73 mV. These traces are from a different recording than was used for *A*. The horizontal scale bar is 200 ms and the vertical scale bar is 4 mV for the intracellular trace. *C*, example of the linear relationship between extracellular and intracellular ripple signals. □, control values; ●, values 20 min following the training protocol. The continuous lines are the best-fitting linear regression lines for each group. The linear relationship was maintained when the two outliers were removed: $r = 0{\cdot}90$ (control), $r = 0{\cdot}85$ (post-training). The dashed lines represent the 99% confidence intervals for the best-fitting lines.

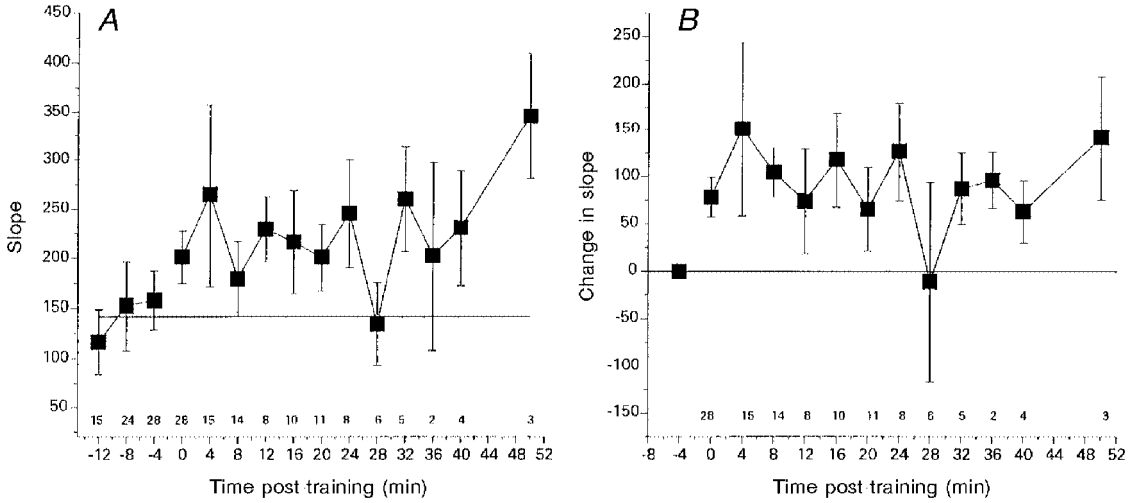

Figure 3. The paired training protocol induces a long-lasting increase in SPW-associated intracellular depolarisations

A, slope values (relationship between integrated extracellular and intracellular signals; arbitrary units) before (12–0 min) and after (0–52 min) pairing SPW activity and intracellular depolarisation. Horizontal line: mean pre-training value. *B*, the data shown in *A* are expressed as a change in slope from the mean baseline slope. Since the number of experiments (*N*) contributing to each time point varied, the actual *N* values are indicated by the small numbers inside the abscissa. The decrease at 28 min is due to a large change in slope in a single rat.

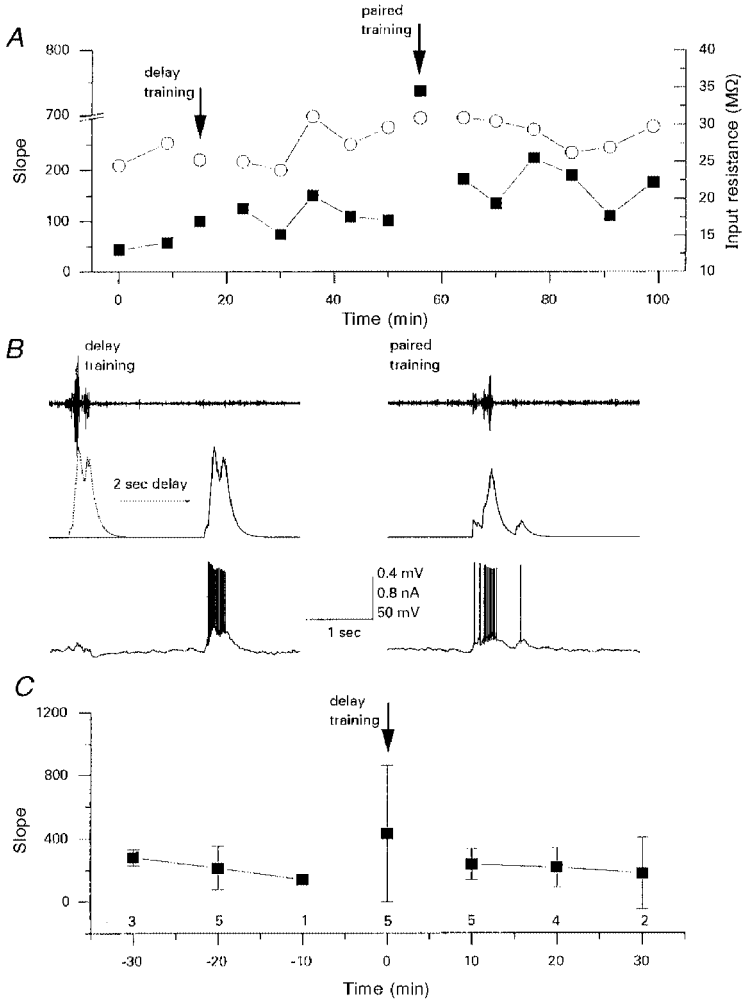

Figure 4. The effect of delayed pairing of extracellular SPW pattern and intracellular depolarisation ('pseudotraining')

A, single experiment. ■, slope values; ○, input resistance. First arrow, delayed training; second arrow, pairing of SPW signal with simultaneous intracellular depolarisation. Changes in the slope are not matched by proportionate changes in input resistance. *B*, delayed training: the extracellular ripple signal was rectified and delayed (2 s) and the derived voltage was used to control intracellular current injection; paired training: the rectified SPW ripple signal was fed back to the recorded cell without delay. *C*, group values for 5 'pseudotraining' experiments demonstrate that delayed training did not produce a significant change in slope, and thus did not change the relationship between extracellular and intracellular signals.

from synchronous interneuron firing. This 'population IPSP' probably reflects the largest component of the current flow during ripples, as indicated by the large extracellular positive waves at times of interneuron discharge (Csicsvari *et al.* 1999). (2) Ripple phase-locked discharge of pyramidal neurons ('mini' population spikes; Buzsáki, 1986; Draguhn *et al.* 1998). Their contribution to the field ripple is relatively small because during a given ripple wave only 2–3 % of pyramidal cells fire together (Csicsvari *et al.* 1998). As in the intracellular experiments, we assumed that an increase in the probability of ripple-related unit discharge, as a result of pairing, reflects an increased responsiveness of the stimulated neurons to an unchanged input during ripples. To control for effects not associated with pairing, we simultaneously monitored the relationship between unit discharge and field ripple in another tetrode. Activity from the non-stimulated tetrode served to normalise data obtained from the stimulated site.

A set of initial experiments was performed to determine the optimal parameters for tetrode stimulation. These showed that currents in the order of 0·5–2 μA were sufficient to activate reliably the cells visible on the tetrode's channels. At these strengths, the amplifiers connected to the electrodes through which current was being passed typically went into overload during the stimulation period. However, the other channels of the tetrode array remained clear, except for an artifact at the start and end of stimulation. Because of the overload, the identity of neuron(s) stimulated could not be unambiguously verified. We assumed that units with the largest amplitude were likely to be stimulated most since the recording/stimulation site was closest to their cell bodies. Consequently, units with large-amplitude spikes were lumped together and the results refer to multi-unit data.

While the rat slept, an initial baseline recording was made of cellular activity during 500 or more SPW events. Stimulation was then applied, with the negative pole of the stimulator connected to the electrode. The following 250 ripples then triggered a stimulation pulse. Immediately after this 'training' period, stimulation was stopped and the SPW-associated cellular activity was recorded in the same way as for the baseline.

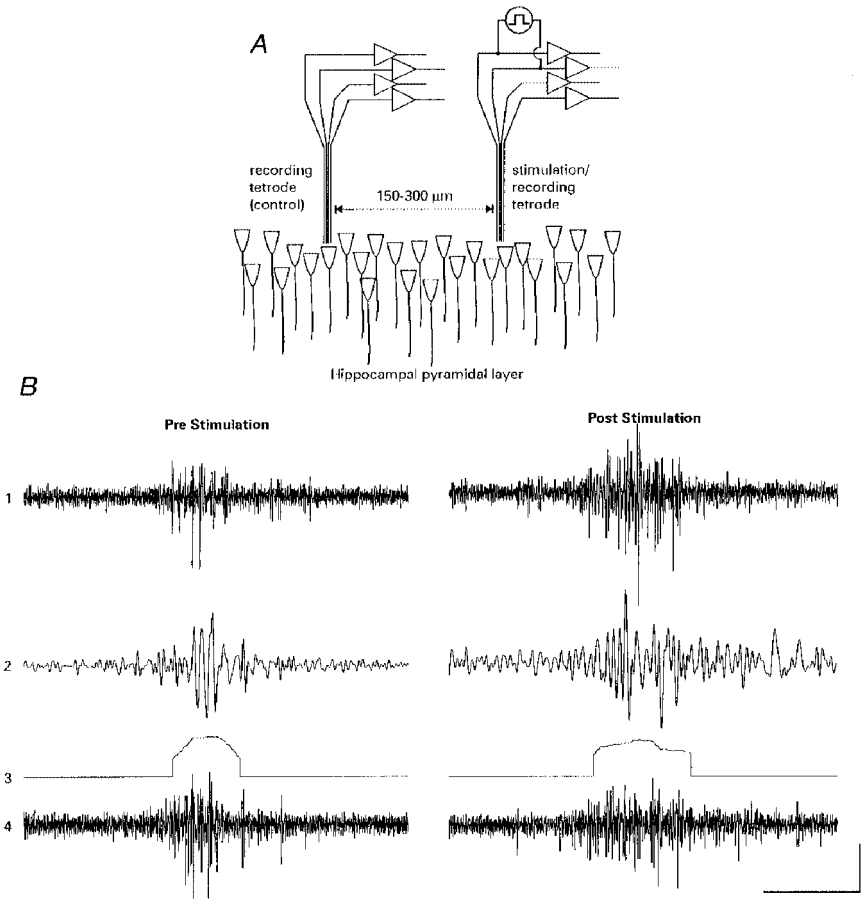

Figure 5. CA1 neuronal activity during sharp waves

A, diagrammatic depiction of the extracellular recording and stimulation system used. *B*, an example of activity pre- (left) and post- (right) stimulation: trace 1, activity of stimulated cells (the figure shows one channel from a tetrode); trace 2, field activity band-pass filtered from 100 to 350 Hz; trace 3, the field activity shown in trace 2 after being filtered and thresholded; trace 4, activity of control cells ~300 μm from stimulation site (again, only one channel from a tetrode is shown). $I_{stim} = 1{\cdot}25$ μA. Calibration bars: 50 ms, 100 μV.

Complete stimulation/recording sessions were performed at 10 sites in seven different animals. An example of the raw results is given in Fig. 5, showing the activity of cells at the experimental and control sites before and after the stimulation. The aggregate results from this session are given in Fig. 6*A*. The slope of the linear regression demonstrated that stimulation led to a significant change in cell activity during ripples (*t* test, $P < 0{\cdot}001$). There was no such change in the activity of the control cell (Fig. 6*B*). For clarity, the data points are binned according to the size of the ripple into groups 0·5 mV ms wide and averaged.

Group data are shown in Fig. 6*C*. In eight of the ten experiments, units recorded by the stimulation/recording tetrode showed a significant increase in ripple-associated activity following 'training' (*t* test, $P < 0{\cdot}01$, mean slope increase $122 \pm 32{\cdot}5\%$) without such a change in the activity of the control cells. In one of the two experiments which did not demonstrate a change, the stimulation tetrode recorded a large-amplitude putative interneuron, as indicated by the high firing rate and spike waveform (Csicsvari *et al.* 1998). No significant changes were found in the length of the ripples following the training protocol (Wilcoxon test).

DISCUSSION

This study has demonstrated that neuronal plasticity can be induced by the Hebbian pairing of stimulation with naturally occurring spontaneous activity patterns in the hippocampus. Enhancement of neuronal responses to hippocampal SPW events were observed in both anaesthetised and freely behaving rats using either intracellular depolarisation of a single cell or juxtacellular stimulation of a small group of neurons.

The basic requirement for Hebbian plasticity, as studied in the long-term potentiation (LTP) protocol (Bliss & Lømo, 1973), is synaptic activation concurrent with postsynaptic depolarisation (Gustafsson & Wigstrom, 1986). Further work has revealed, however, that the temporal pattern of synaptic activation may have significant effects on the induction of plasticity (Larson *et al.* 1986; Dudek & Bear, 1992; Markram & Tsodyks, 1996; Dobrunz & Stevens, 1999). The conclusion follows that, in order to explore fully the relationship between LTP and memory, it is necessary to study the plasticity evoked in response to naturally occurring input patterns (Cruikshank & Weinberger, 1996;

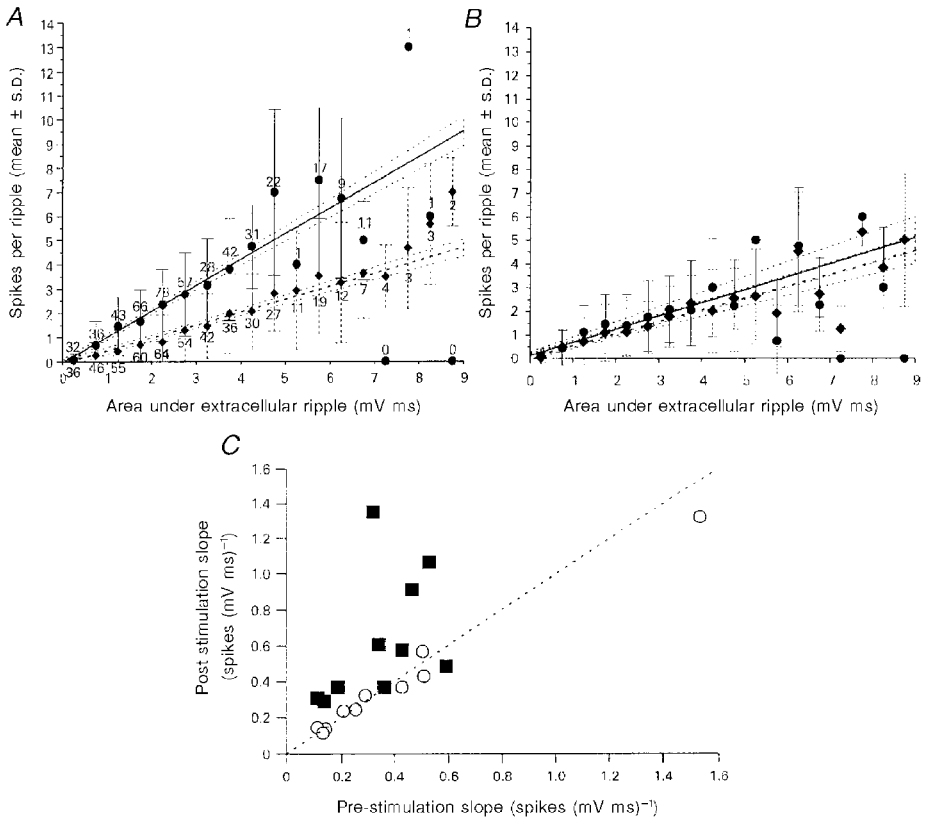

Figure 6. Ripple-associated activity for the cells shown in Fig. 5

A demonstrates data for the site of stimulation and *B* demonstrates data from the control site. Ripple amplitude was estimated by integrating the area under the curves shown in trace 3 of Fig. 5*B* and the number of spikes fired during each ripple was determined using spike clustering. The resultant data were grouped by ripple amplitude into bins 0·5 mV ms wide (◆, pre-stimulation; ●, post-stimulation, ± S.D.). The dashed (pre-stimulation) and continuous (post-stimulation) lines show the linear regression fit together with 99% confidence bands. The number of data points in each bin is shown by the numerals against each point in *A*, and is identical for the data shown in *B*. *C*, the slope pre- (*x*-axis) and post- (*y*-axis) stimulation: ■, stimulated; ○, control.

Rogan *et al.* 1997; Stevens, 1998). While this may be accomplished using sensory stimulus-evoked responses in the neocortex, the hippocampus, which is a common preparation for LTP research, does not exhibit simple sensory responses (Ranck, 1973). Hippocampal SPWs, however, represent a naturally occurring spontaneous activity pattern, whose physiological characteristics correlate well with those necessary for LTP (Buzsáki, 1989; Kamondi *et al.* 1998). Although any role of SPWs in memory remains to be determined, SPWs do represent a good candidate for the investigation of naturally occurring synaptic plasticity.

The design of the present study was based on two assumptions. First, that participation of CA3 pyramidal cells in an SPW event is not random but certain subpopulations dominate (Buzsáki, 1989; Ylinen *et al.* 1995). Second, that the probability of participation of a given CA1 pyramidal cell in an SPW event is determined by the efficacy of CA3–CA1 synapses (Liao *et al.* 1992; Rosenmund *et al.* 1993; Allen & Stevens, 1994). The Schaffer collateral from a single CA3 cell innervates more than half the longitudinal length of CA1 (Ishizuka *et al.* 1990; Li *et al.* 1994) and the collaterals exhibit a high degree of convergence and divergence. Approximately 8–18% of CA1 pyramidal cells fire during any one particular SPW and the probability of participation in successive SPW events varies from 0 to 40% for a given pyramidal cell (Ylinen *et al.* 1995; Csicsvari *et al.* 1999). A prediction from these previous observations is that increasing the synaptic weights between an arbitrarily chosen CA1 pyramidal cell and its presynaptic (Schaffer) inputs would increase the SPW-associated depolarisation and discharge probability. The results appear to support these assumptions. The enhanced SPW participation of the pyramidal neuron(s) after training suggests that synaptic modification occurred in the CA3–CA1 (Schaffer) synapses. A potential objection against this conclusion is that extracellular stimulation in the CA1 area runs the risk of triggering antidromic spikes in the Schaffer collaterals and artificially firing CA3 cells, thus altering the input pattern under study. However, intensities of 25–100 μA are required to produce unitary EPSCs in CA1 cells from stimulation of Schaffer collaterals (Bolshakov *et al.* 1997). In our study, the stimulation electrode was placed very close to the cell bodies, an area free of Schaffer collateral terminals. The current intensities used represent the lower range of those shown to be effective in stimulating neocortical neurons (Stoney *et al.* 1968). Importantly, the results of the intracellular experiments exclude the possibility of altering the CA3 recurrent circuitry.

Measurement of the altered functional connectivity was based on the observed linear relationship between the magnitude of the SPW ripple and either cellular depolarisation or cellular output of a small neuronal aggregate. The extracellularly recorded ripple is a combination of alternating currents represented by interneuron-mediated somatic hyperpolarisation of pyramidal cells and the summed extracellular spikes of pyramidal cells (Buzsáki, 1986; Ylinen *et al.* 1995). This combined effect may be reflected by the intracellular response, which is a sum of EPSPs and IPSPs. Similarly, the probability of the extracellular unit discharge summed across a small population of neurons reflects afferent depolarisation (Schaffer collaterals) and locally generated feedforward and feedback inhibition.

A further issue concerns the actual nature of the potentiation observed here. The most widely studied form of LTP in the CA1 region is synapse specific and dependent on calcium influx through NMDA receptors (Collingridge *et al.* 1983; Lynch *et al.* 1983). Induction of this form of LTP would imply that that the pairing protocol used here selected a subset of the synapses active during SPWs in general and that the efficacy of this subset was potentiated, resulting in an increased response to further SPW-associated excitatory volleys. An alternative explanation for the extracellular results is that the enhancement observed here was related to EPSP spike potentiation (Jester *et al.* 1995). In such a case, the paired stimulation would simply have resulted in an enhanced response to input at all synapses, even those inactive at the time of stimulation. While the stimulation protocol used here did not result in a simple change in the overall excitability of the cell, it is possible that the change in membrane resistance played a role in the mediation of the effects. Further studies will be required to determine whether the effect we have observed is dependent on the synapse-specific entry of calcium through NMDA channels.

In summary, our findings demonstrate that naturally occurring patterns are a useful means to measure the input–output transformation in hippocampal networks. Furthermore, consistent pairing of a natural input and postsynaptic activation of a single cell or small groups of cells by local microstimulation can bring about plastic changes in cellular response profiles. This approach may therefore provide interesting possibilities for testing theories of hippocampal function.

Allen, C. & Stevens, C. F. (1994). An evaluation of causes for unreliability of synaptic transmission. *Proceedings of the National Academy of Sciences of the USA* **91**, 10380–10383.

Barnes, C. A. (1995). Involvement of LTP in memory: are we 'searching under the street light'? *Neuron* **15**, 751–754.

Bliss, T. V. & Collingridge, G. L. (1993). A synaptic model of memory: long-term potentiation in the hippocampus. *Nature* **361**, 31–39.

Bliss, T. V. & Lømo, T. (1973). Long-lasting potentiation of synaptic transmission in the dentate area of the anaesthetized rabbit following stimulation of the perforant path. *Journal of Physiology* **232**, 331–356.

Bolshakov, V. Y., Golan, H., Kandel, E. R. & Siegelbaum, S. A. (1997). Recruitment of new sites of synaptic transmission during the cAMP-dependent late phase of LTP at CA3-CA1 synapses in the hippocampus. *Neuron* **19**, 635–651.

Brown, T. H., Kairiss, E. W. & Keenan, C. L. (1990). Hebbian synapses: biophysical mechanisms and algorithms. *Annual Review of Neuroscience* **13**, 475–511.

Buzsáki, G. (1986). Hippocampal sharp waves: their origin and significance. *Brain Research* **398**, 242–252.

Buzsáki, G. (1989). Two-stage model of memory trace formation: a role for 'noisy' brain states. *Neuroscience* **31**, 551–570.

Buzsáki, G., Haas, H. L. & Anderson, E. G. (1987). Long-term potentiation induced by physiologically relevant stimulus patterns. *Brain Research* **435**, 331–333.

Buzsáki, G., Horváth, Z., Urioste, R., Hetke, J. & Wise, K. (1992). High-frequency network oscillation in the hippocampus. *Science* **256**, 1025–1027.

Buzsáki, G., Leung, L.-S. & Vanderwolf, C. H. (1983). Cellular basis of hippocampal EEG in the behaving rat. *Brain Research Reviews* **6**, 139–171.

Collingridge, G. L., Kehl, S. J. & McLennan, H. (1983). Excitatory amino acids in synaptic transmission in the Schaffer collateral–commissural pathway of the rat hippocampus. *Journal of Physiology* **334**, 33–46.

Cruikshank, S. J. & Weinberger, N. M. (1996). Evidence for the Hebbian hypothesis in experience-dependent physiological plasticity of neocortex: a critical review. *Brain Research Reviews* **22**, 191–228.

Csicsvari, J., Hirase, H., Czurko, A. & Buzsáki, G. (1998). Reliability and state dependence of pyramidal cell-interneuron synapses in the hippocampus: an ensemble approach in the behaving rat. *Neuron* **21**, 179–189.

Csicsvari, J., Hirase, H., Czurko, A., Mamiya, A. & Buzsáki, G. (1999). Oscillatory coupling of hippocampal pyramidal cells and interneurons in the behaving rat. *Journal of Neuroscience* **19**, 274–287.

Dobrunz, L. E. & Stevens, C. F. (1999). Response of hippocampal synapses to natural stimulation patterns. *Neuron* **22**, 157–166.

Draguhn, A., Traub, R. D., Schmitz, D. & Jefferys, J. G. (1998). Electrical coupling underlies high-frequency oscillations in the hippocampus *in vitro*. *Nature* **394**, 189–192.

Dudek, S. M. & Bear, M. F. (1993). Bidirectional long-term modification of synaptic effectiveness in the adult and immature hippocampus. *Journal of Neuroscience* **13**, 2910–2918.

Gustafsson, B. & Wigstrom, H. (1986). Hippocampal long-lasting potentiation produced by pairing single volleys and brief conditioning tetani evoked in separate afferents. *Journal of Neuroscience* **6**, 1575–1582.

Ishizuka, N., Weber, J. & Amaral, D. G. (1990). Organization of intrahippocampal projections originating from CA3 pyramidal cells in the rat. *Journal of Comparative Neurology* **295**, 580–623.

Jester, J. M., Campbell, L. W. & Sejnowski, T. J. (1995). Associative EPSP–spike potentiation induced by pairing orthodromic and antidromic stimulation in rat hippocampal slices. *Journal of Physiology* **484**, 689–705.

Kamondi, A., Acsady, L. & Buzsáki, G. (1998). Dendritic spikes are enhanced by cooperative network activity in the intact hippocampus. *Journal of Neuroscience* **18**, 3919–3928.

Kelso, S. R., Ganong, A. H. & Brown, T. H. (1986). Hebbian synapses in hippocampus. *Proceedings of the National Academy of Sciences of the USA* **83**, 5326–5330.

King, C. & Buzsáki, G. (1998). Combined extracellular recording and microstimulation of single cells in the behaving rat. *Society for Neuroscience Abstracts* **24**, 362.17.

Larson, J., Wong, D. & Lynch, G. (1986). Patterned stimulation at the theta frequency is optimal for the induction of hippocampal long-term potentiation. *Brain Research* **368**, 347–350.

Li, X. G., Somogyi, P., Ylinen, A. & Buzsáki, G. (1994). The hippocampal CA3 network: an *in vivo* intracellular labeling study. *Journal of Comparative Neurology* **339**, 181–208.

Liao, D., Jones, A. & Malinow, R. (1992). Direct measurement of quantal changes underlying long-term potentiation in CA1 hippocampus. *Neuron* **9**, 1089–1097.

Lynch, G., Larson, J., Kelso, S., Barrionuevo, G. & Schottler, F. (1983). Intracellular injections of EGTA block induction of hippocampal long-term potentiation. *Nature* **305**, 719–721.

Markram, H. & Tsodyks, M. (1996). Redistribution of synaptic efficacy between neocortical pyramidal neurons. *Nature* **382**, 807–810.

Morris, R. G. & Frey, U. (1997). Hippocampal synaptic plasticity: role in spatial learning or the automatic recording of attended experience? *Philosophical Transactions of the Royal Society* B **352**, 1489–1503.

Ranck, J. B. (1973). Studies on single neurons in dorsal hippocampal formation and septum in unrestrained rats. I. Behavioral correlates and firing repertoires. *Experimental Neurology* **41**, 461–531.

Rogan, M. T., Stäubli, U. V. & Ledoux, J. E. (1997). Fear conditioning induces associative long-term potentiation in the amygdala. *Nature* **390**, 604–607.

Rosenmund, C., Clements, J. D. & Westbrook, G. L. (1993). Nonuniform probability of glutamate release at a hippocampal synapse. *Science* **262**, 754–757.

Stevens, C. F. (1998). A million dollar question: does LTP = memory? *Neuron* **20**, 1–2.

Stoney, S. D., Thompson, W. D. & Asanuma, H. (1968). Excitation of pyramidal tract cells by intracortical microstimulation: effective extent of stimulating current. *Journal of Neurophysiology* **31**, 659–669.

Wigstrom, H., Gustaffson, B., Huang, Y. Y. & Abraham, W. C., (1986). Hippocampal long-term potentiation is induced by pairing single afferent volleys with intracellularly injected depolarizing current pulses. *Acta Physiologica Scandinavica* **126**, 317–319.

Ylinen, A., Soltesz, I., Bragin, A., Penttonen, M., Sik, A. & Buzsáki, G. (1995). Intracellular correlates of hippocampal theta rhythm in identified pyramidal cells, granule cells, and basket cells. *Hippocampus* **5**, 78–90.

Acknowledgements

This work was supported by NIH (NS34994, MH54671) and the Epilepsy Foundation of America.

Corresponding author

G. Buzsáki: Center for Molecular and Behavioural Neuroscience, Rutgers University, 197 University Avenue, Newark, NJ 07102, USA.

Email: buzsaki@axon.rutgers.edu

Author's present address

X. Leinekugel: Inserm U 29, Maternité de Port-Royal, Paris 75014, France.